XVIII IMEKO WORLD CONGRESS
Metrology for a Sustainable Development
September, 17 – 22, 2006, Rio de Janeiro, Brazil

A PC-CONTROLLED REFLECTOMETER FOR FUNCTIONAL IMAGING OF OCULAR FUNDUS

Matteo Bonaiuti[1], *Luigi Rovati*[1] *and Charles Riva*[2]

[1] Department of Information Engineering, University of Modena and Reggio Emilia, Modena, Italy, rovati.luigi@unimo.it
[2] Ophthalmology Unit, University of Bologna, Bologna, Italy

Abstract: The paper presents an imaging reflectometer designed to detect flicker-induced reflectance changes of the ocular fundus. The system is based on a modified fundus camera completely controlled by a personal computer via USB interface.
The system allows in-vivo functional imaging of the ocular fundus in the near-infrared region with flicker light stimulus in the visible spectrum.

Keywords: Reflectometry, near-infrared functional imaging, ocular fundus imaging.

1. INTRODUCTION

Ocular fundus reflectometry is a method for determining the distribution of pigments at the eye retina. This non-invasive analysis is known to be useful for diagnostic investigations [1]. The basic idea derives from a standard modus operandi of ophthalmologists to observe the color distribution of the ocular fundus to identify possible retinal pathologies as well as effects of laser therapy. The reflectance, which is directly observable in the visible spectrum, is mainly determined by melanin molecules. Nevertheless, in the range 540nm-700nm additional contributions come from haemoglobin and thus from blood that provides nutriments and oxygen to retinal neural molecules. The contribution of haemoglobin to the absorption becomes relatively more relevant in the near-infrared region (NIR: 700nm-1000nm) where direct observation by ophthalmologists is not possible. Nevertheless, this spectral region can be easily explored by means of a CCD or Vidicon camera.

Changes in the near-infrared absorption during neural activities have been observed in the cortex [2]. These changes are the results of the variations in blood volume and blood oxygenation required to support neural activities. Similar mechanisms have been observed in the peripapillary retinal tissues and optic disc during diffuse flicker stimulation [3]. These functional changes have been studied by means of ocular fundus reflectometry at 569 and 600nm.

In this paper, to investigate in humans the variations of reflectivity of the ocular fundus due to physiological changes induced by flicker stimulation, a new PC-controlled NIR reflectometer is presented. Since NIR light is used to illuminate the eye fundus, pupillary dilatation is not needed, if the measurements are taken in a dark environment.

2. METHODS

To perform accurate analyses of the reflectance properties of the ocular fundus, besides a suitable instrumentation, an adequate theoretical description of the interaction between radiation and retinal tissues is required. Therefore, before introducing the developed system, in the next section we introduce a theoretical description of the problem.

2.1 *Basic theory*

Neurovascular coupling in the retinal tissues is a mechanism which adjusts local tissue oxygenation to the increased metabolic needs induced by the neural activity associated with vision. The application of a diffuse luminance flicker causes a variation in retinal blood volume which in turn induces modifications in light-absorption properties of the tissues [3]. These variations can be detected as changes in the tissue's reflectance.

The light impinging the fundus is transmitted by the retina and choroid, it is reflected by the sclera and then transmitted again by the choroid and retina to reach the observer. Thus the fundus reflectance is given by

$$R(\lambda) = R_{sclera}(\lambda) \cdot 10^{-2\ OD_{tot}(\lambda)} \quad , \tag{1}$$

where R_{sclera} (λ) is the reflectance of the sclera, and OD_{tot} (λ) can be evaluated as:

$$OD_{tot}(\lambda) = 2.2 \cdot \left(\mu_{ar}(\lambda) \cdot t_r + \mu_{ac}(\lambda) \cdot t_c\right) . \tag{2}$$

Here $\mu_{ar}(\lambda)$ and $\mu_{ac}(\lambda)$ are the absorption coefficients of the neural retina and choroid of thickness t_r and t_c respectively.

This simple model does not take into account the effects of the reflection due to the interface between vitreous humor and neural retina [4]. Also the absorption/reflection of the RPE-receptors complex is neglected [5]. Nevertheless, since in our study we are interested in variations induced by stimuli, these steady-state contributions are not relevant.

The information of interest is contained in the changes of $\mu_{ar}(\lambda)$ and $\mu_{ac}(\lambda)$ induced by alterations in blood oxygenation during neural activities.

2.2 Instrumentation

The developed system is based on a commercial fundus camera (TRC-WT, Topcon, Japan) properly modified. Consider the simplified optical layout shown in Fig. 1. The standard illumination lamp was removed and, in the same plane of the lamp filament, we inserted the NIR LED L1 (LED770-03AU, Roithner Lasertechnik, Austria). The light emitted by the green LED L2 (Kingbright, Taiwan) is diffused by the diffuser D and focused on the same path of the NIR beam emitted by L1. The illuminated field at the fundus is confocally imaged onto the sensitive area of the CCD video camera VC (LDH0702/20, Philips, Holland). The NIR light illuminates the ocular fundus at a specific wavelength, i.e. 770nm ± 20nm. The imaging filter F (RT-830, Edmund Optics GmbH, Germany) transmits this NIR light and blocks the flicker green radiation, thus the image acquired by the B&W camera VC contains the NIR reflectance information. Filter F has a center-wavelength of 830nm and a FWHM of 260nm.

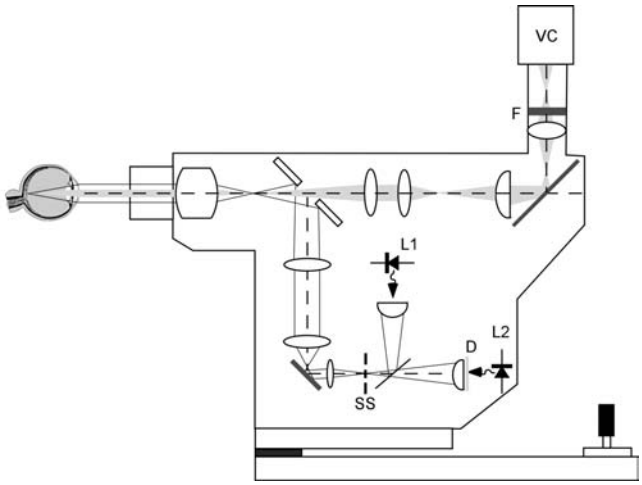

Fig. 1. Simplified optical layout of the modified fundus camera. VC: High sensitivity video camera, L1: NIR LED, L2: Flicker LED, D: diffuser, F: imaging filter and SS: slit stop.

The LEDs L1 and L2 are controlled by a personal computer via the USB port whereas the images generated by VC are synchronously acquired using a standard frame grabber board. A specific application in Visual Basic software has been developed to control the LEDs and to perform image acquisition tasks. Therefore, all in the functional imaging experiments can be controlled by means of a batch program running onto a PC.

Fig. 2 shows the circuit diagram of the LED-driving system. L1 and L2 are driven by the adjustable constant currents I1 and I2, respectively generated by the voltage-controlled current sources VCCS1 and VCCS2. The currents I1 and I2 are proportional to the control voltages V1 and V2 which are provided by the DAC subsystem D. This network is based upon an octal digital-to-analog converter which allows calibration of both depth of modulation and LED currents. The calibration constants are stored into the non-volatile memory M and are sent to the D/A converters at the power-up. Both D and M are accessed to by the micro-controller unit C via a two-wire I^2C synchronous serial bus. The communication between the personal computer and the LED-driving system is performed by means of the full-speed USB interface peripheral of subsystem C. An application-specific firmware for the micro-controller C has been developed .

The NIR LED current I1 can be adjusted in the range 0mA to 100mA in 256 steps to control the emitted optical power and therefore the brightness of the fundus images acquired by the VC camera. I2 can be modulated by the signal VF to obtain the flicker effect of L2. The time-base of the flicker stimulus consists of a 16-bit timer peripheral onboard the micro-controller C. Our driver allows an adjustable duty cycle in the range 0 to 100%, 0.5 to 20 Hz modulation frequency and a depth of modulation in the range 0 to 100%. Fig. 3 shows a picture of the resulting measuring system.

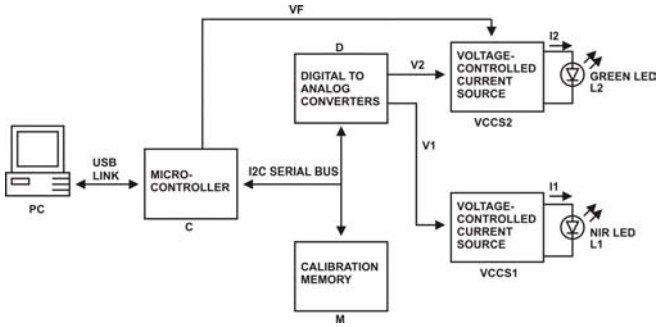

Fig. 2. Block diagram of the LED-driving circuit. The LED currents I1 and I2 are generated by the DAC subsystem D that is controlled by the micro-controller C interfaced to the personal computer PC by means of the full-speed USB link.

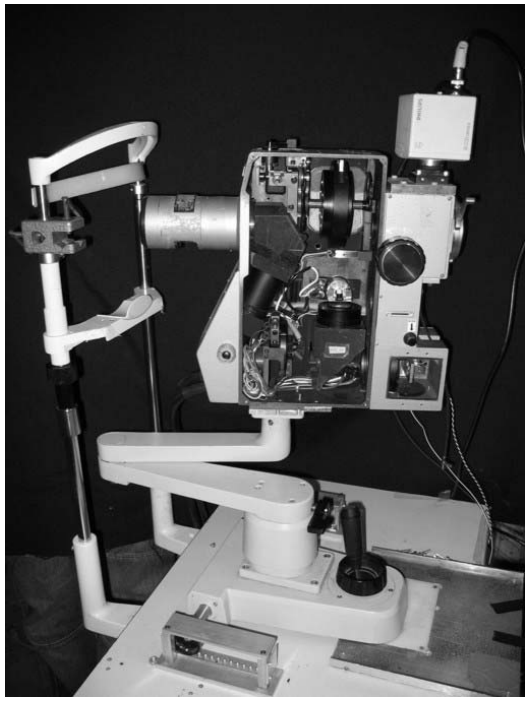

Fig. 3. Picture of the measuring system. The different optical components are easily identifiable comparing the picture with the drawing reported in Fig. 1 .

2.3 Calibration

To determine the actual reflectance of the fundus important parameters such as the emission spectrum of the illumination source, the spectral response of the CCD elements and the chromatic effects of the optics must be taken into account. Thus, we perform a calibration of the measuring system on two targets with known reflectance characteristics. The first calibration target is a diffuse reflector with reflectance 99 ± 4% from 250 to 2500 nm (Spectralon SRS-99-020, Labsphere, USA). Moreover, to compensate the stray-light effects, a dark reference measurement is performed with a black cloth. The reference targets are placed on the bottom of a mechanical eye model (Topcon, Japan) in order to replace the phantom fundus.

The actual fundus reflectance is calculated as:

$$R(\lambda) = \frac{I_f(\lambda) - I_d(\lambda)}{I_w(\lambda) - I_d(\lambda)} \quad , \qquad (3)$$

where $I_f(\lambda)$ is the intensity signal measured at the ocular fundus, whereas $I_w(\lambda)$ and $I_d(\lambda)$ are the intensity signals measured with the diffuse reflector and with the black cloth.

3. RESULTS AND DISCUSSION

The fundus camera system has been first assembled and the optical paths of the beams have been verified. Then the basic blocks of the PC LED driving circuits have been verified and tested in operation and the performance of the LED sources have been verified. Preliminary measurements have been performed in-vivo on a adult volunteer. Major results obtained during these characterization activities are reported in the following sections.

3.1 System characterization

Since reflectance measurements on the eye fundus are wavelength-dependent, the emission spectra of the illumination sources L1 and L2 have been first measured using a photonic multichannel analyzer (C5966, Hamamatsu Photonic K.K., Japan). The obtained data are shown in Fig. 4 for both L1 and L2. Table 1 shows relevant characteristics of LEDs L1 and L2 obtained from data shown in Fig. 4.

The current injected into both the LEDs L1 and L2 can be varied digitally in 256 steps by a software control panel. Thus the calibration and the linearity test of each of the chromatic channels is required to determine the actual power emitted by the LEDs. Optical power measurements were taken at the reflectometer's output on the plane of the target cornea using a PC-controlled optical power meter (SH-TO-USB, Ophir Optronics, Israel) equipped with an optical head (PD300-UV-SH, Ophir Optronics, Israel).

Fig. 5 shows the optical power emitted by LED L1 as a function of the digital codes.

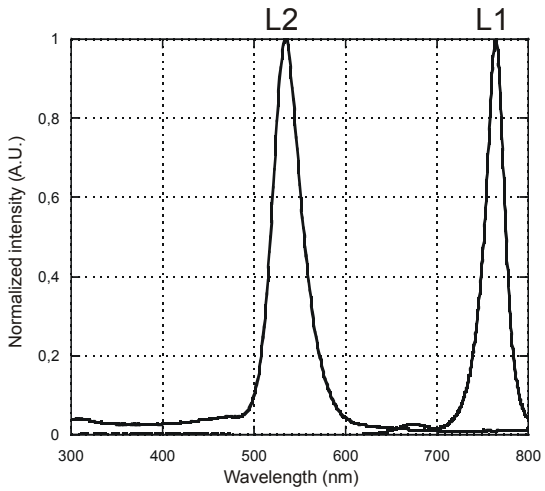

Fig.4. Emission spectra of the flicker (L2: $\overline{\lambda} = 535nm$) and NIR (L1: $\overline{\lambda} = 770nm$) LED.

Table 1. Measured peak wavelength and full-width half maximum of the emission spectra of LEDs L1 and L2.

	L1	**L2**
Peak Wavelength	765nm	535nm
FWHM	24nm	37nm

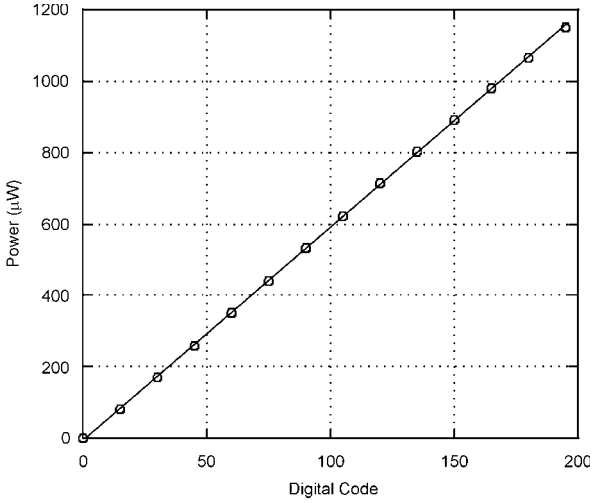

Fig. 5. Calibration curve of the 770nm light source. Experimental points (o) and linear fit (straight line) are plotted.

For each digital value, 60 optical power readings were taken with an 1-second time interval between samples. Then the samples were averaged and the result was plotted as a circle in Fig. 7.

The experimental data were then fitted with a straight line minimizing the least square errors, obtaining the following linear calibration equation:

$$\widetilde{P}_{770} = -5.1263 + 5.9575 D_{in} \quad (\mu W) \, , \qquad (4)$$

where $\widetilde{P}_{770}$ is the interpolated emitted power and D_{in} is the digital code transmitted to the driver. The fitting procedure exhibits a linear correlation coefficient R=0.99996.
The value of the integral non-linearity (INL) of the calibration curve was calculated according the following definition:

$$INL_{\%,FSR} = \sqrt{\frac{\sum_{i=1}^{N}\left(P_i - \widetilde{P}_i\right)^2}{N-1}} \cdot \frac{100}{FSR}, \qquad (5)$$

where N is the number of experimental points involved in the calculation, P_i is the optical power measured at the i-th digital code, $\widetilde{P}_i$ is the optical power as calculated from Eq. (5), and FSR is the optical power's dynamic range evaluated by varying D_{in} from 195 and 0. Thus the INL value obtained for the NIR channel is 0.292%.
Fig. 6 shows the calibration curve obtained for the flicker optical source. Measurements have been performed following the same protocol implemented for the NIR channel.

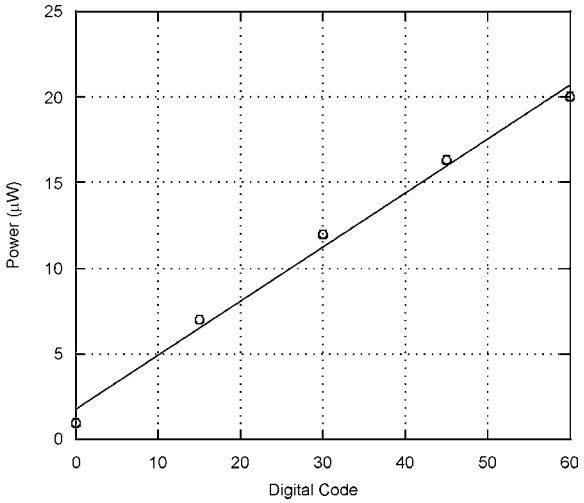

Fig. 6. Calibration curve of the 535nm light source. Experimental points (o) and linear fit (straight line) are plotted.

Thus the linear calibration equation of the flicker channel is:

$$\widetilde{P}_{535} = 1.8 + 0.31553 D_{in} \quad (\mu W). \qquad (6)$$

In this case the linear correlation coefficient is R=0.99547, whereas the INL is 3.76%. Note that the FSR of the flicker channel was defined varying D_{in} from 60 and 0.

The design of the networks VCCS1 and VCCS2 was aimed to obtain a stable emission from LEDs L1 and L2, since fluctuations of the light emitted by these sources induce errors in the reflectance measurements and changes in the optical stimuli. To test the performance of the realized sources the warm-up time and the long term stability have been measured for both the LEDs L1 and L2.

Fig. 7 shows a 60-minute recording of the optical power at the reflectometer output when only L1 is turned on. The optical power was measured on the plane of cornea and the sampling time interval was set to 30s. The programmable current source was set to a digital value of 50 out of 255, corresponding to a current of 22.89mA injected in L1. This current was measured using a 6 ½-digit DMM (34401A, Hewlett-Packard, USA). A statistical analysis performed on the acquired data after a warm-up time of t=1020s yielded an optical power, in terms of mean value ± standard deviation, of 290.01±0.08μW.

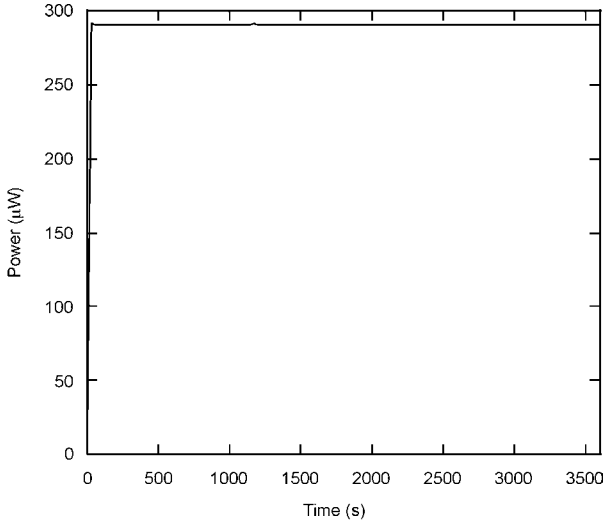

Fig. 7. Emitted optical power from the reflectometer when the NIR LED is turned on at time t=0s.

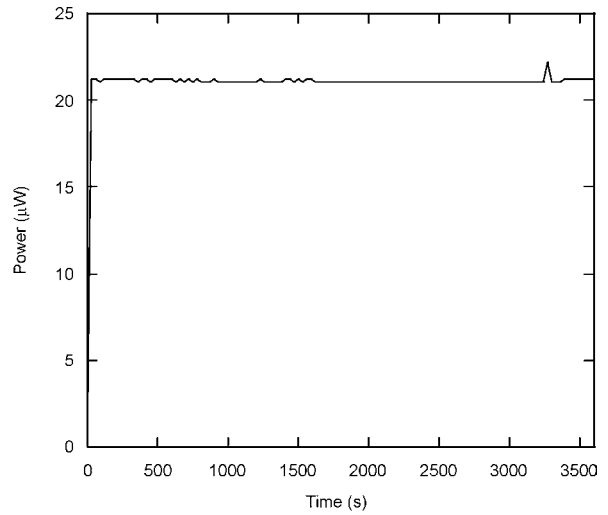

Fig. 8. Emitted optical power from the reflectometer when the Flicker LED is turned on at time t=0s.

Fig. 8 shows a 60-minute recording of the optical power at the reflectometer output when only L2 is turned on. In this case the current injected into the LED L2 was 5mA. The recording protocol was the same as for the 770nm source. A statistical analysis performed on the acquired data after a warm-up time of t=1800s yielded an optical power, in terms of mean value ± standard deviation, of 21.13±0.14μW.

Thus the warm-up time for the whole illumination system was considered to be equal to the higher one of the two sources, i.e. 1800s.

3.2 Preliminary acquired images

Preliminary in-vivo measurements have been acquired on a 67 years old male subject. Informed consent was obtained from the subject. The instrument was placed in a dark environment and separated from the light of the monitor of the personal computer and the operator controlling the reflectometer by means of a thick black cloth. Images of the ocular fundus were taken setting the NIR power impinging the subject's cornea to 440μW. The observation angle was approximately 20°. Duration of the recording was 2s. Fig. 9 shows the ocular fundus images centered at the optic disk and acquired with the instrument from the volunteer. Each picture has a resolution of 640h x 480v pixels.

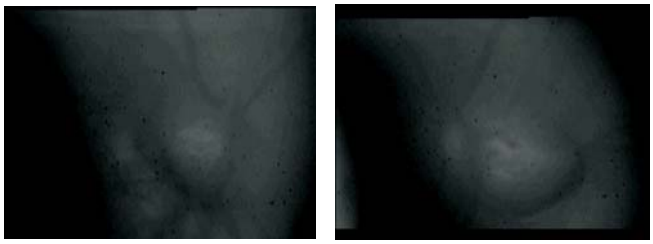

(a) (b)

Fig. 9. Fundus images of the subject's left (a) and right (b) eyes.

4. CONCLUSIONS

The paper presents a novel imaging reflectometer completely controlled by a personal computer. Preliminary results on a volunteer are encouraging and show that the system is suitable to acquire images of the ocular fundus. Moreover, thanks to the flicker channel, the system could be used to study the retinal haemodynamics which support the flicker-induced neural activities.

ACKNOWLEDGMENTS

The authors gratefully acknowledge the Fondazione Cassa di Risparmio in Bologna, Italy, that partially supported the research activity presented in this paper.

REFERENCES

[1] T.J.M. Berendshot, P.J. DeLint, and D. van Norren, "Fundus reflectance-historical and present ideas," Progr. Ret. Eye Res. Vol. 22, pp. 171-200, 2003.

[2] L. Rovati, S. Fonda, L. Bulf, R. Ferrari, G. Biral, G. Salvatori, A. Bandera, and M. Corradini, "Functional cerebral activation detected by an integrated system combining CW-NIR spectroscopy and EEG", Proc. SPIE Vol. 5326, pp. 118-125, 2004.

[3] M. Crittin, and C.E. Riva, "Functional imaging of the human papilla and peripapillary region basd on flicker-induced reflectance changes," Neurosci. Lett. Vol. 360, pp. 141-144, 2004.

[4] W.A.H. Rushton, "Straylight and the measurement of the mixed pigment in the retina," J. Physiol. 176, pp. 46-55, 1965.

[5] F.C. Delori, and K.P. Pfibsen, "Spectral reflectance of the human ocular fundus," Appl. Opt. 28, 1061-1077, 1989.